

# Effect of crack depth on fracture toughness of 20MnMoNi55 pressure vessel steel

N. Narasaiah\*, S. Tarafder, S. Sivaprasad

Materials Science Technology Division, National Metallurgical Laboratory, Burmahines (Council of Scientific & Industrial Research), Jamshedpur 831007, Jharkhand, India

## ARTICLE INFO

### Article history:

Received 23 September 2009

Received in revised form 3 December 2009

Accepted 4 December 2009

### Keywords:

Fracture toughness

Stretch zone width

Constraint effect

20MnMoNi55 steel

## ABSTRACT

Ductile fracture behaviour of 20MnMoNi55 steel under quasi-static loading has been studied using single-edge notched bend specimens. To understand the influence of crack depth on fracture behaviour,  $J$ – $R$  curves were obtained from specimens pre-cracked to various  $a/W$  in the range of 0.25–0.75, in steps of approximately 0.1. Stretch zone width dimensions were measured on the fractured surfaces of the broken specimens. The stretch zone dimensions that were determined have been used in conjunction with the experimentally derived  $J$ – $R$  curves to obtain a value of the ductile fracture toughness parameter  $J_{SZW}$ . The initiation toughness,  $J_i$ , at the intersection of the blunting line and the power-law fit to the  $J$ – $R$  curve, and the critical toughness,  $J_c$ , following the ASTM standard, were estimated. Comparisons of  $J_{SZW}$  with  $J_i$  and  $J_c$  have been made for 20MnMoNi55 steel as a function of the  $a/W$  ratio. The  $J_i$  and  $J_c$  values are found to be higher at lower  $a/W$ , i.e. under low constraint, and decrease with increasing  $a/W$ . It is observed that  $J_{SZW}$  is not affected by  $a/W$ , and that its value is lower bound to  $J_i$  and  $J_c$  values of the material investigated.

© 2010 Elsevier B.V. All rights reserved.

## 1. Introduction

Determination of initiation fracture toughness in ductile materials is not straightforward. Unlike in brittle materials, where the point of crack initiation is easily detectable due to sharp changes in the load carrying capacity, ductile materials will experience sufficient crack tip blunting prior smooth transition from crack tip blunting process to tearing. Often these series of events pose difficulty in pin-pointing the crack initiation stage. The process may be further complicated due to variation of constraint attending crack tips. Fracture behaviour of ductile materials is usually characterized by elastic–plastic fracture parameters such as the  $J$ -integral, stretch zone width, crack tip opening displacement, etc. The variations in these parameters with variation in constraint are often difficult to rationalize, particularly from the point of view that these parameters are employed to represent material behaviour that are deemed to be universal, largely independent of test and specimen parameters. Often, the fracture resistance of materials obtained from testing standard specimens is not applicable to the fracture of components made of that material due to the difference in the constraint or triaxiality conditions at the tip of the crack in the two cases [1]. An attempt has been made to understand the nature of variation of fracture resistance parameters with change in crack depth (i.e. with variation of constraint) in a pressure vessel piping material.

In ductile materials, fatigue pre-crack usually gets blunt on the application of load to accommodate plastic strains arising out of the local deformation processes at the crack tip. On continuation of loading, the blunting at the crack tip increases and reaches a limiting size, governed by the deformation capacity of the material, and further initiates fracture (ductile crack) at its tip. On a ductile fracture surface, crack tip blunting is manifested as a featureless region known as the stretch zone. The stretch zone that forms during the process of ductile fracture can be thought of as a frozen imprint of the state of deformation at the instant of the critical event of ductile crack extension. Its extent can thus be used as a marker to indicate the corresponding fracture toughness parameter from the experimental resistance curve [2–5]. The effect of variation of constraint on the fracture toughness metrics thus determined has also been investigated in the present work. The suitability of the parameters to represent the fracture toughness of materials, irrespective of the constraint condition, to which cracks in these specimens are subjected, is discussed.

## 2. Material and experimental details

The material used in this investigation is 20MnMoNi55 pressure vessel application steel. The steel was in the form of rectangular blocks having 135 mm width and 70 mm thick. The nominal composition of the material is given in Table 1. Fig. 1 shows the typical microstructure of the investigated steel in which bainite is distributed in the ferritic matrix. Table 2 lists the mechanical properties of the material obtained from tensile tests at room temperature. The tensile flow curves of the steel exhibited prominent yield-point effect.

\* Corresponding author. Tel.: +91 657 2345187; fax: +91 657 2345213.

E-mail addresses: [narasaiah@yahoo.co.in](mailto:narasaiah@yahoo.co.in), [nn@nmlindia.org](mailto:nn@nmlindia.org) (N. Narasaiah).

**Table 1**  
Compositions of investigated steel (in weight percentage).

Material	Elements							
	C	Mn	Si	S	Mo	Cr	Ni	Balance
20MnMoNi55	0.2	1.25	0.3	0.005	0.5	0.17	0.6	Fe

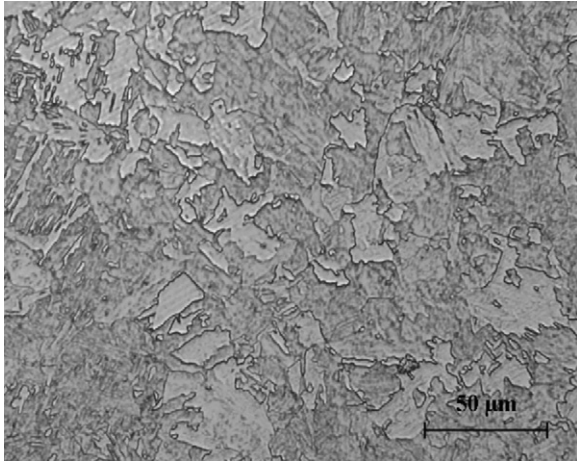


**Fig. 1.** Typical microstructure of the investigated steel.

Single-edge notched bend (SENB) specimens, of 20 mm thickness  $B$  and 50 mm width  $W$ , were employed for carrying out monotonic single-specimen  $J$ - $R$  tests at room temperature. For studying constraint effects on ductile fracture behaviour, SENB specimen geometry was preferred to avoid the distortion that occur at the loading holes of the compact tension (CT) geometry at lower initial crack lengths. All specimens were machined with integral knife-edges on their front face for compliance based crack length measurement, and were side-grooved after fatigue pre-cracking to ensure planar fracture. Specimens were fatigue pre-cracked under decreasing  $\Delta K$  envelopes in servo-hydraulic testing system interfaced to computers for test control and data acquisition. Pre-cracks ( $a$ ) of various extents were incorporated in the specimens to vary the crack tip constraint.

The single-specimen technique was employed for generating  $J$ - $R$  curves as per the procedures laid down in ASTM standard E1820 [6]. The loading scheme for this technique consisted of ramping pre-cracked specimens at a rate of  $3 \times 10^{-3}$  mm/s through constant incremental displacements, followed by unloading and then reloading through 50% of the incremental displacement at the same rate, and repeating the sequence till substantial crack extension had taken place through ductile tearing. The typical load–displacement records that results due to implementation of this scheme for 20MnMoNi55 steel at two  $a/W$  ratios are shown in Fig. 2.

The crack length ( $a$ ) at each instance of unloading was calculated from the elastic compliance ( $C$ ) of the unloading curve using compliance crack length relations of the form:

$$\frac{a}{W} = f(u), \quad u = \frac{1}{\sqrt{EB_{eff}C + 1}} \quad (1)$$

**Table 2**  
Tensile parameters of investigated steel at room temperature.

Material	YS (MPa)	UTS (MPa)	$e_u$ (%)	$e_t$ (%)	RA (%)
20MnMoNi55	489.9	620.5	9.51	23.04	68.65

YS: yield strength, UTS: ultimate tensile strength,  $e_u$ : uniform elongation,  $e_t$ : total elongation, RA: reduction in area.

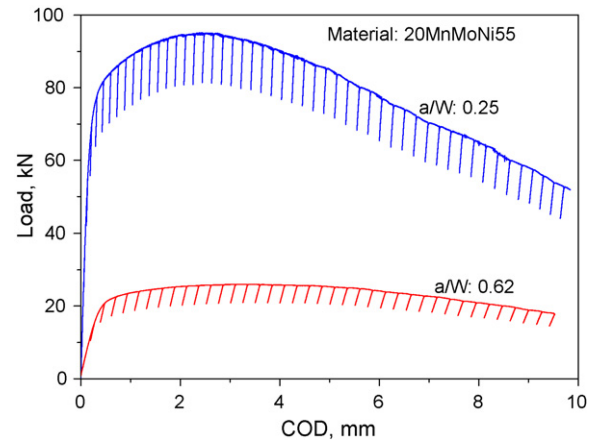


**Fig. 2.** Typical load–displacement records obtained during  $J$ - $R$  testing at different  $a/W$  ratios for 20MnMoNi55 steel.

where  $E$  is the elastic modulus and  $f$  is a polynomial function. The energy parameter  $J$  for the instant of  $i$ th unloading was calculated incrementally using:

$$J_i = \frac{K_i^2(1 - \nu^2)}{E'} + J_{pl(i)} \quad (2a)$$

$$J_{pl(i)} = \left( J_{pl(i-1)} + \frac{\eta_{(i-1)}(A_{pl(i)} - A_{pl(i-1)})}{b_{(i-1)}B_N} \right) \left( 1 - \frac{\gamma_{(i-1)}(a_i - a_{(i-1)})}{b_{(i-1)}} \right) \quad (2b)$$

where  $A_{pl(i)} - A_{pl(i-1)}$  = incremental plastic area;  $b_i = (W - a_i)$ .

In the above equations,  $K_i$  is the stress intensity factor, calculated from the instantaneous load  $P_i$  and the crack length  $a_i$ ;  $\nu$  is the Poisson's ratio;  $\eta$  and  $\gamma$  are the geometry and crack length dependent factors; and  $B_N$  is the net specimen thickness obtained after side grooving. The second term in Eq. (2b) represents the correction proposed by James and Richard [7] to account for crack extension in the loading step. The factors  $\eta$  and  $\gamma$  in Eq. (2b) are dependent on crack length and were obtained from relations given by Sumpter [8]. This is necessary when lengths of pre-cracks are varied through a large range in order to study constraint effects on ductile fracture.

The load, displacement and crack mouth opening displacement (CMOD) data obtained from ductile fracture tests were analysed post-test, employing inhouse-developed software to obtain a set of  $J$  and crack extension ( $\Delta a$ ) data pairs to construct the  $J$ - $R$  curves. The software adopted iterative procedures to obtain the experimental blunting line slope  $m$ , the power-law representation of the tearing part of the resistance curve, and the adjusted initial crack length ( $a_{oq}$ ). This ensured that subjectivity in determination of critical parameters such as the fracture toughness  $J_i$ , obtained at the departs of the power-law tearing curve from the blunting line, or the critical fracture toughness  $J_c$ , identified from the point where an offset of the blunting line at  $\Delta a = 0.2$  mm intersects the tearing curve, was eliminated.

Fractured surfaces carefully extracted from the tested specimens were examined in SEM such that the plane of fracture was aligned to be normal to the electron beam. At this  $0^\circ$  tilt position, stretch features were recorded at a sufficiently high magnification (at the order of 100–500 $\times$ ) to be able to identify local features within the stretch zone, while ensuring that the whole width of the stretch zone was contained in the field of view. Care was taken to obtain a good contrast, so that stretch zone limits could be demarcated easily. The stretch zone boundaries were traced on captured SEM images and approximately 25 measurements were made for each of the two fracture surfaces obtained from a specimen. Large number of measurements were required so that the variation in

Download English Version:

<https://daneshyari.com/en/article/1579836>

Download Persian Version:

<https://daneshyari.com/article/1579836>

[Daneshyari.com](https://daneshyari.com)